Solar and Stellar Flares and their Effects on Planets
Proceedings IAU Symposium No. 320, 2015
A.G. Kosovichev, S.L. Hawley & P. Heinzel, eds.

doi:10.1017/S1743921316000508

Thermal characteristics of a B8.3 flare observed on July 04, 2009

Arun Kumar Awasthi[1], **Barbara Sylwester**[2], **Janusz Sylwester**[2] **and Rajmal Jain**[3]

[1]Astronomical Institute, University of Wroclaw, Poland
email: arun.awasthi.87@gmail.com

[2]Space Research Center of Polish Academy of Sciences, Wroclaw, Poland
email: bs@cbk.pan.wroc.pl, js@cbk.pan.wroc.pl

[3]Kadi Sarva Vishwavidyalaya, Gandhinagar, India
email: rajmal_9@yahoo.com

Abstract. We explore the temporal evolution of flare plasma parameters including temperature (T) - differential emission measure (DEM) relationship by analyzing high spectral and temporal cadence of X-ray emission in 1.6-8.0 keV energy band, recorded by SphinX (Polish) and Solar X-ray Spectrometer (SOXS; Indian) instruments, during a B8.3 flare which occurred on July 04, 2009. SphinX records X-ray emission in 1.2-15.0 keV energy band with the temporal and spectral cadence as good as 6 μs and 0.4 keV, respectively. On the other hand, SOXS provides X-ray observations in 4-25 keV energy band with the temporal and spectral resolution of 3 s and 0.7 keV, respectively. We derive the thermal plasma parameters during impulsive phase of the flare employing well-established Withbroe-Sylwester DEM inversion algorithm.

Keywords. Sun: corona, Sun: flares, plasmas, Sun: X-rays, radiation mechanisms: thermal, techniques: spectroscopic.

1. Introduction

Thermal characteristics of solar flare plasma employing the multi-wavelength observations is of immense interest as it can shed light on the ongoing coupling processes in solar atmosphere. In particular, X-ray emission during a flare is the best probe of various thermal and non-thermal energy release processes (Brown (1971)). Generally, flare plasma parameters viz. temperature (T), emission measure (EM), etc. are derived by forward-fitting/inversion of the observed X-ray spectrum (Jain *et al.* (2011)). However, the spectroscopic inversion of X-ray emission is an ill-posed problem, leading to substantial uncertainties in the derived T and EM values (Craig & Brown (1976)). Moreover, several different DEM inversion techniques, with various functional dependence of DEM on T viz. power-law, single-gaussian etc., are used to interpret observed X-ray spectrum. Further, Withbroe-Sylwester (W-S) DEM inversion algorithm (Sylwester, Schrijver, & Mewe (1980), Kepa *et al.* (2008)) provides a more general scheme for such studies.
Therefore, in this paper, we present the analysis of X-ray emission observed during a B8.3 flare occurred on July 04, 2009, the only event recorded in common with Solar X-ray Spectrometer (SOXS; Jain *et al.* (2005)) and Solar Photometer in X-rays (SphinX; Gburek *et al.* (2013)). Section 2 presents the observations while data analysis and results are given in Section 3. Section 4 presents the summary and conclusions.

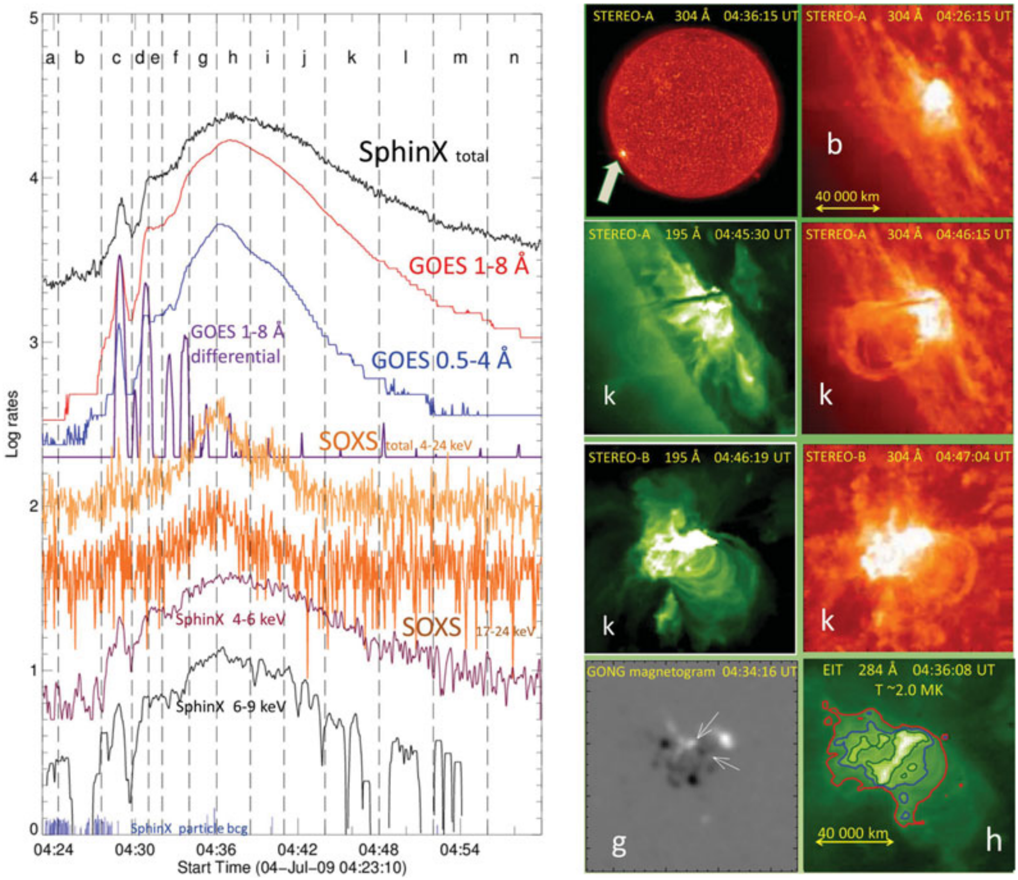

Figure 1. Left Panel: Temporal evolution of X-ray emission as recorded by SphinX, SOXS and *GOES* during SOL2009-07-04T04:37 (B8.3) flare. Dotted bars show the time intervals for which spectral analysis is undertaken. Right Panel: Multi-wavelength overview of the flare from *STEREO-A* and *STEREO-B* and EIT/*SOHO*. Activity areas are shown by arrows in the GONG Magnetogram (bottom).

2. Observations

We study a B8.3 flare event of July 04, 2009, which occurred in active region 11024. Thermal characteristics of the flare plasma are derived by analyzing X-ray spectra in 1.6-5.0 keV and 5.0-8.0 keV energy bands, recorded by SphinX and SOXS, respectively. Temporal evolution of X-ray emission during the flare as observed by SphinX and SOXS instruments as well as by *GOES* is shown in the left panel of the Fig. 1. Further, morphological evolution of the flaring region is studied from the EUV images obtained from *STEREO-A, B* and Extreme Ultraviolet Imager Telescope (EIT) onboard *SOHO* mission, as shown in the right panel of the Fig. 1.

3. Thermal characteristics of the flare plasma

We analyze the X-ray spectra, recorded during the flare, with the help of W-S *DEM* inversion method (Sylwester, Schrijver, & Mewe (1980)). This numerical method employs maximum likelihood approach in which a $DEM-T$ distribution and hence corresponding theoretical spectrum is derived in an iterative manner with the aim to minimize its

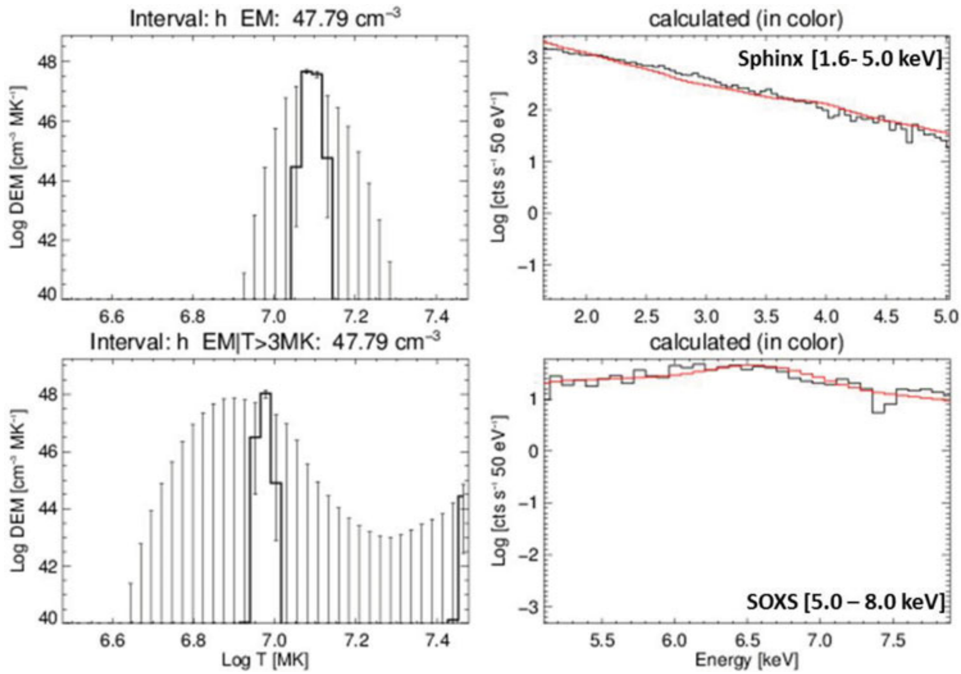

Figure 2. Top row: Best-fit *DEM-T* relationship as well as the spectral-fit (drawn by red color) employing W-S inversion algorithm for the emission in 1.6-5.0 keV (plotted by black color), recorded by SphinX during 04:36:00-04:38:30 UT. Bottom row: Best-fit *DEM-T* and fitted SOXS spectrum in 5.0 - 8.0 keV for the aforesaid time duration.

difference with the input observed spectrum (Kepa *et al.* (2008)). Coronal abundances are adopted from CHIANTI atomic database (Del Zanna *et al.* (2015)) while deriving the shape of theoretical spectra. As an input to this method, we have used fluxes recorded in the 73 energy bins (corresponding to the energy band 1.6-5.0 keV) and 35 energy bins (corresponding to the energy band 5.0-8.0 keV) by SphinX and SOXS instruments, respectively. The X-ray spectra are analyzed for various time duration as shown by dotted lines in the left panel of Fig. 1. Top row of the Fig. 2 shows the best-fit $DEM-T$ relation derived by analyzing X-ray spectrum in 1.6-5.0 keV (low-energy), observed by SphinX during the peak of the impulsive phase of the flare, 04:36:00-04:38:30 UT. Similarly, in the bottom panel, we present the best-fit $DEM-T$ curve and spectral-fit over the X-ray spectrum in 5.0-8.0 keV (high-energy), observed by SOXS during the aforesaid time.

From Fig. 2, it may be noted that the best-fit $DEM-T$ relation derived from SphinX observation suggests nearly isothermal nature of the DEM, with the peak at temperature $(T_p)\sim$ 13 MK. Similarly, the best-fit DEM to the SOXS spectrum in 5.0-8.0 keV energy band for the same time interval suggests isothermal nature in the form of single gaussian function dependence on T, however, at T_p = 9.8 MK. Next, thermal energy are derived from the best-fit $DEM-T$ curve of Sphinx and SOXS observations and estimated to be 5.1 and 3.6 $\times$ 10^{29} ergs, respectively. We employ the volume estimated from EIT/*SOHO* EUV wavelength images as shown in Fig. 1 for the calculation of thermal energies.

4. Summary and Conclusions

We study the thermal characteristics of the plasma during SOL2009-07-04T04:37 (B8.3) flare by analyzing its X-ray spectrum in various energy bands, as obtained by

SphinX and SOXS instruments. We summarize the preliminary findings of this study as follows:

(*a*) Emission-measure is found to be of isothermal nature during the peak of the impulsive phase of the flare.

(*b*) Thermal energy and the temperature estimated by analyzing low-energy (from SphinX) and high-energy (from SOXS) bands within SXR spectrum result in different peak temperature as well as thermal energy.

In the next step, we have made a detailed investigation of thermal characteristics as well as the evolution of *DEM-T* relationship in various phases of the flare by combining the observations from SphinX and SOXS instruments. The corresponding paper is under review in the ApJ Main Journal (Awasthi *et al.* (2016)).

Acknowledgements

This research has been supported by Polish grant UMO-2011/01 /M/ST9/06096. Moreover, the research leading to these results has received funding from the European Community's Seventh Framework Programme (FP7/2007-2013) under grant agreement no. 606862 (F-CHROMA).

References

Awasthi, A. K., Sylwester, B., Sylwester, J., & Jain, R. 2016, *Submitted to the ApJ*

Brown, J. C. 1971, *Solar Phys.*, 18, 489.

Craig, I. J. D. & Brown, J. C. 1976, *A&A*, 49, 239.

Del Zanna, G., Dere, K. P., Young, P. R., Landi, E., & Mason, H. E. 2015, *A&A*, 582, A56

Gburek, S., Sylwester, J., Kowalinski, M., Bakala, J., Kordylewski, Z., Podgorski, P., Plocieniak, S., Siarkowski, M., Sylwester, B., Trzebinski, W., Kuzin, S. V., Pertsov, A. A., Kotov, Y. D., Farnik, F., Reale, F., & Phillips, K. J. H. 2013, *Solar Phys.*, 283, 631.

Jain, R., Awasthi, A. K., Rajpurohit, A. S., & Aschwanden, M. J. 2011, *Solar Phys.*, 270, 137.

Jain, R., Dave, H., Shah, A. B., Vadher, N. M., Shah, V. M., Ubale, G. P., Manian, K. S. B., Solanki, C. M., Shah, K. J., Kumar, S., Kayasth, S. L., Patel, V. D., Trivedi, J. J., & Deshpande, M. R. 2005, *Solar Phys.*, 227, 89.

Kepa, A., Sylwester, B., Siarkowski, M., & Sylwester, J. 2008, *Adv. Sp. Res.*, 42, 828.

Sylwester, J., Schrijver, J., & Mewe, R. 1980, *Solar Phys.*, 67, 285